LASER INTERFEROMETER GRAVITATIONAL WAVE OBSERVATORY

LIGO Laboratory / LIGO Scientific Collaboration

LIGO- T040027-01-R | *LIGO* | 19th November 2007

Conceptual Design of Beamsplitter Suspension for Advanced LIGO

Norna A Robertson and Mark Barton

Distribution of this document:
LIGO Science Collaboration

This is an internal working note
of the LIGO Project.

California Institute of Technology
LIGO Project – MS 18-34
1200 E. California Blvd.
Pasadena, CA 91125
Phone (626) 395-2129
Fax (626) 304-9834
E-mail: info@ligo.caltech.edu

Massachusetts Institute of Technology
LIGO Project – NW17-161
175 Albany St
Cambridge, MA 02139
Phone (617) 253-4824
Fax (617) 253-7014
E-mail: info@ligo.mit.edu

LIGO Hanford Observatory
P.O. Box 1970
Mail Stop S9-02
Richland WA 99352
Phone 509-372-8106
Fax 509-372-8137

LIGO Livingston Observatory
P.O. Box 940
Livingston, LA 70754
Phone 225-686-3100
Fax 225-686-7189

http://www.ligo.caltech.edu/

1 Introduction

This is an update (rev -01) of the original conceptual design document (entitled "Design of Beamsplitter Suspension for Advanced LIGO") from 9th February 2004. That document presented the case for making the beamsplitter suspension a triple pendulum rather than a quadruple pendulum as used for the ETMs and ITMs. A conceptual design based on the size of beamsplitter at that time (350 mm diameter by 60 mm thick) was presented and curves for predicted seismic isolation performance and thermal noise were given. It was shown that these met the noise requirements for the beamsplitter. The thermal noise curve was produced assuming that the beamsplitter was suspended by four silica fibres of circular cross-section.

Since that design was put together several factors have changed:

a) The beamsplitter (BS) size has been increased to 370 mm diameter x 60 mm thick. Currently it is expected to have a wedge angle of 0.9^{o}. This diameter has been shown to have sufficient free aperture to give an acceptable level of optical loss with or without flats on the side– see G070471-00-E for information on losses with flats.

b) A reassessment of the need for silica fibres has taken place (see discussion below).

3) The decision has been taken that the design of the BS and folding mirror (FM) suspensions should be the same.

2 Beamsplitter Requirements

Currently the noise requirement at 10 Hz from the sum (suitably added) of BS optics axis motion and vertical motion is 2e-17 m/rt Hz (see the cavity optics noise requirements document T010007-02 and ref P Fritschel, e-mail 27 Jan 2004). See version 00 of the conceptual design document for fuller discussion. The consideration of whether steel wires can be used in place of fused silica fibres hinges on how much coupling from vertical into longitudinal motion of the BS occurs, and this is linked to the orientation of its wedge angle. See section 4 for a full discussion. The conclusion from these considerations is that the suspension will be on steel wires.

3 Choice of Parameters

The original working design which was investigated was of a triple suspension with approximately equal masses (12.7 kg for the original size of BS) and equal wire lengths of 60 cm at each stage. The choice of equal masses and equal wire lengths as a baseline has come from experience with previous designs and leads to good coupling of modes. In addition using three equal lengths gives the best isolation for a given overall length. The overall length was chosen to satisfy the available length for a beamsplitter suspension in a BSC (noting that this was at that time expected to be 70 mm longer than for an ETM) *prior* to considerations to reduce the overall length of BSC suspension structures as summarized in T040028-00. Since then the recommendations on length in T040028 have been adopted, and the decision to make the FM the same design as the BS has been taken. Since the FM must necessarily be very close to the same length as an ITM (they are adjacent to each other and the laser beam is close to horizontal), this implies that for a common BS/FM design, the choice for the length of the BS or FM is now such that the BS, FM and ITM mirror centres are the same distance from the optics table. Note that this doesnt imply that the suspension lengths will necessarily be the same. The distance between the top suspension point and the optics table above need not be the same. For the current beamsplitter design length see Appendix C.

3.1 More on parameter set (added Sept 2007 and further updated November 2007)

Several revisions to the parameter set have been made since the first draft of this document was produced in July 2007. See Appendix C for an update and for the latest (at the time of writing) full parameter set.

4 Suspension Thermal Noise

In the 2004 design, the final stage of the suspension consisted of 4 silica fibres of circular cross-section, 140 micron radius (stress ~500 MPa) and 60 cm length. This gave a highest vertical frequency of 10.9 Hz and a first violin mode at 400 Hz, which satisfied the requirements expressed in the document on low-frequency cut-off (P Fritschel et al T020034-00-D), which requires a vertical mode of 12 Hz or lower, and first violin mode 400 Hz or higher. The noise spectrum (see rev 00 of this document) showed the x noise alone lies well below the requirement at 10 Hz. The overall noise is dominated by the z (vertical) contribution up to around 20 Hz. The spectrum assumed coupling at the level of 0.001 of vertical added in quadrature to the horizontal. At 10 Hz the overall noise is below the requirement by a factor of 10, at a value of 2.0×10^{-18} m/√ Hz, with a narrow spike of higher noise around 11 Hz at the vertical resonance. That frequency could be pushed below 10 Hz to 8.9 Hz using a radius of fibre of 113 micron (stress ~770 MPa).

There are compelling reasons to consider changing from silica wire to steel wire if it gives acceptable performance. The use of steel gives a significant reduction in complexity of design and construction. The key issue is how much vertical thermal noise is coupled in, since (as noted above) in the 10 to 20 Hz region it is vertical thermal noise which dominates.

Using a revised set of parameters (new size of beamsplitter, shorter overall length, minor changes to wire spacing and wire radii to allow for larger BS) the following thermal noise curves were produced by Mark Barton using his Mathematica model of a triple pendulum. The full parameter list from his model used to produce figures 1, 2 and 3 is included in Appendix B.

Firstly in figure 1 we see the thermal noise estimate with silica fibres assuming 0.001 vertical coupling. As expected the target of 2 x 10^-17 m/rt Hz at 10 Hz is comfortably met, with noise at 10 Hz, which is dominated by the vertical component, at around 10^-18 m/rt Hz. If larger coupling of 0.01 is assumed this raises the level an order of magnitude – still within the noise requirement.

In figure 2 we see the thermal noise estimate using steel wires, again assuming 0.001 vertical coupling. The target noise requirement at 10 Hz of 2 x 10^-17 m/rt Hz is met. Around 10 Hz the dominant noise is the horizontal component. However the highest vertical mode at ~ 16.4 Hz can be seen rising up above the horizontal.

In figure 3 we see the thermal noise estimate using steel wires and a larger vertical coupling of 0.01. In this case the vertical dominates the horizontal at all frequencies from 10 Hz and the high frequency trend extrapolated back to 10 Hz comes in at just above 2x10^-17 m/ rt Hz.

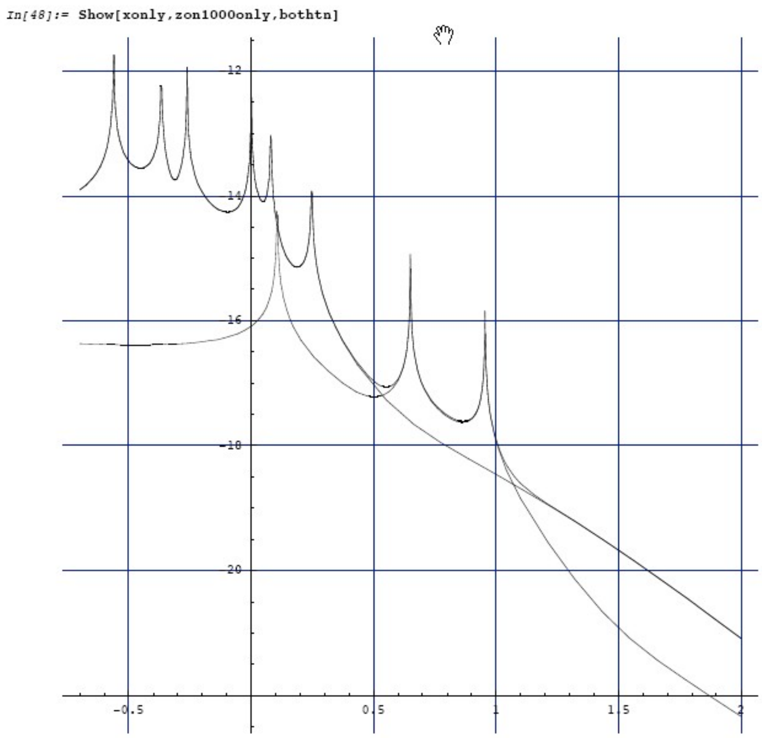

Figure 1. Thermal noise for BS on silica fibres, parameters as in Appendix B. Assumes 0.001 z coupling.

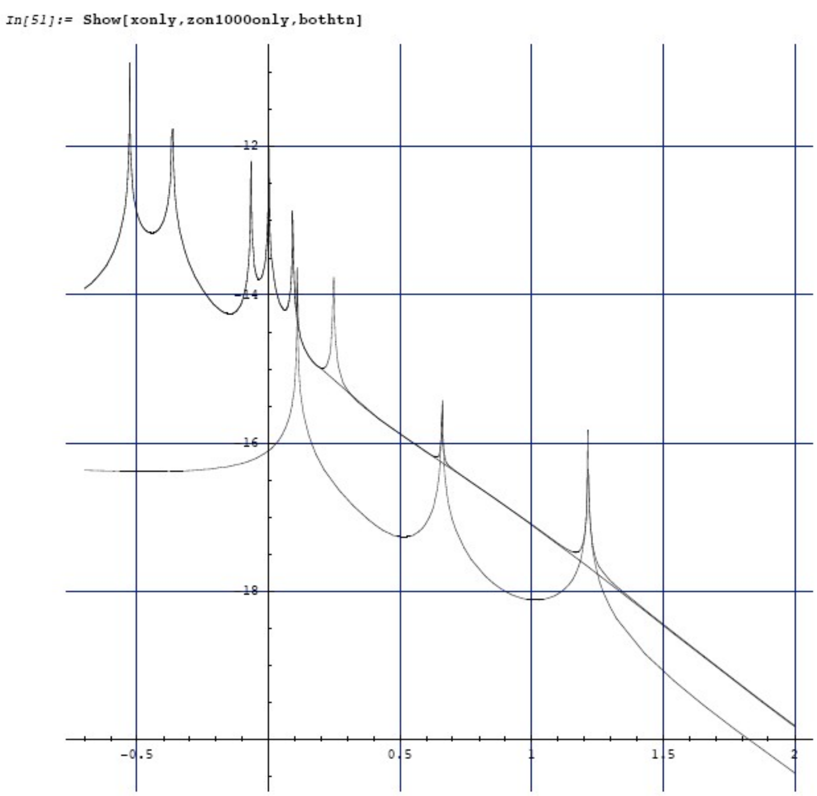

Figure 2. Thermal noise for BS on steel wires, parameters as in Appendix B. Assumes 0.001 z coupling.

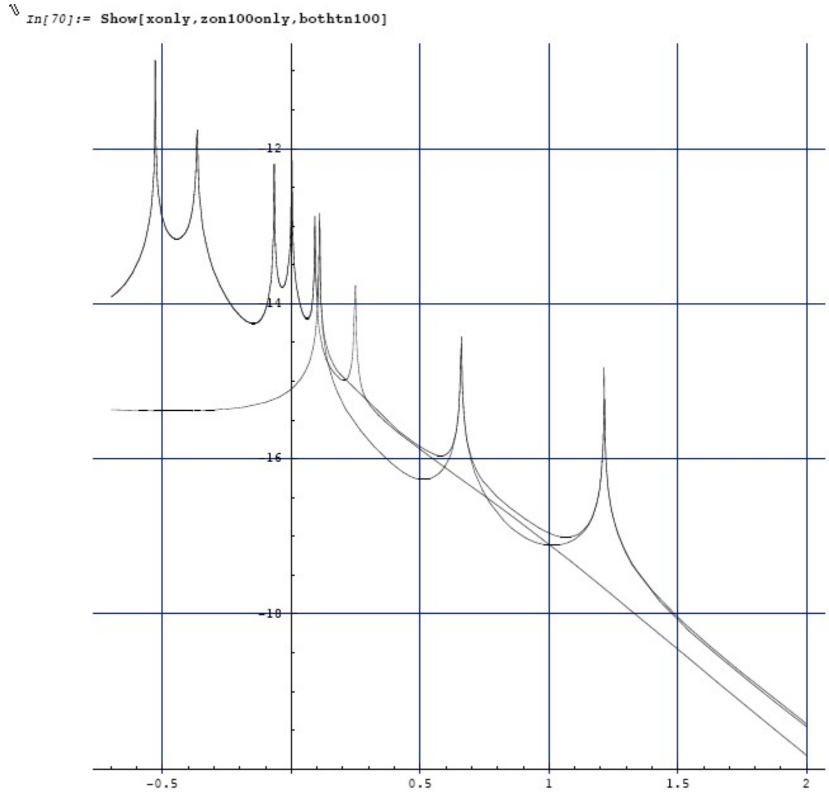

Figure 3. Thermal noise for BS on steel wires, parameters as in Appendix B. Assumes 0.01 z coupling.

In summary, silica fibres clearly meet the noise requirement whether the vertical coupling is 0.001 or 0.01 and also satisfy that the highest vertical mode is below 10 Hz.

With steel wires and a coupling of 0.001 the noise requirement is met except for the peak at the highest vertical mode (~ 16.4 Hz for this parameter set). If it is acceptable to have such a peak then steel wires could be used. With steel wires and a coupling of 0.01 the noise requirement is barely met.

If a vertical wedge is used in the BS the vertical coupling could be as great as 0.01. In that case it appears that steel wires would not be a good choice. Thus the use of a horizontal wedge has been considered. Such an orientation would imply less vertical coupling (0.001 or less) and hence make steel still a good option. A horizontal wedge produces some coupling of roll into longitudinal but this can be completed removed by moving the spot on the mirror from the centre to the sweet spot (the new centre of mass). This has been shown using Mark Barton's Mathematica model, see figures 4, 5, 6 and 7. Figures 4 and 5 are for the beam hitting the centre of the mirror with 0.001 and 0.01 vertical coupling respectively. Figures 6 and 7 are for the beam hitting the sweet spot (2.1 mm from the centre for the particular parameter set used). Note that these figures were produced for a slightly different parameter set to the graphs shown in figures 1, 2, and 3, (parameters as at 18th July). This accounts for the slightly different mode frequencies for the vertical and roll modes. In other respects these graphs are very similar to the vertical ones except for the appearance of the roll mode when not hitting the sweet spot.

In conclusion it looks like steel wires are acceptable with a horizontal wedge (for which orientation vertical coupling is expected to be ~ 0.001), and so the baseline has been changed to steel wires as captured in RODA M070120-02.

5 Seismic Isolation, Mode Frequencies and Damping

The longitudinal and vertical transfer functions derived from the MATLAB model of the beamsplitter for the parameter set given in appendix A are shown in figures 8 and 9. The mode frequencies are also given in the appendix. There are minor differences in the parameter set used to generate these graphs compared to the thermal noise curves given in section 4. The longitudinal transfer function (with damping time ~10 secs) has a magnitude at 10 Hz of ~1.9 x 10^{-6}. This, combined with active platform noise level of 2 x 10^{-13} m/√ Hz at 10 Hz, gives a noise level at the optic of ~3.8x10^{-19} m/√ Hz at 10 Hz. The vertical transfer function is ~1.2 x10^{-2} at 10 Hz (with damping time ~4 secs), giving vertical noise level at optic of ~2.4x10^{-15} m/√ Hz. Including a 10^{-3} coupling factor gives a residual noise level in the horizontal due to vertical motion of 2.4 x 10^{-18} m/√ Hz. Taking the quadratic sum of these numbers yields a total essentially the same as the noise due to vertical alone, and lying well below the requirement. However note that if the coupling were 0.01, the seismic noise due to vertical coupling into horizontal would not meet the noise requirement.

6 Other Noise Sources

Using the MATLAB model we can also estimate the magnitude of pitch and yaw contributions. The larger of these transfer functions at 10 Hz is for yaw, at ~8 x 10^{-6}. Assuming an angular input at the platform of around 2 x 10^{-13} rad/√Hz and a 1mm beam offset we find a horizontal noise level of 2 x 10^{-21} m/√Hz at 10 Hz, negligible compared to the requirement.

A further consideration is that of noise introduced by local control. A combination of steep electronic filtering and some eddy current damping (ECD) should yield a workable solution. In fact ECD could comfortably be used without any active control for some modes, and ECD is being incorporated into the design. It has been checked that the thermal noise associated with using ECD is below the noise requirement for the beamsplitter – see Appendix C.

7 Conclusions

We have investigated the use of a triple pendulum suspension for the beamsplitter and conclude that it appears to satisfy the noise requirements. The use of steel wires instead of silica fibres has been studied with respect to suspension thermal noise considerations and it is concluded that using steel wires in combination with a horizontal wedge gives acceptable performance.

The latest parameter set at the time of finishing this revision (01) of the document (November 2007) is given in Appendix C. However it should be noted that this is still a conceptual design. Detailed design is currently being carried out and these parameters should only be taken as a guide to the likely final set.

x thermal noise at the centre of the face for beamspitter with steel wires and 0.9° symmetric horizontal wedge rotated so that the front face is +x (20070718bswireHWsymrot), broken down by components: direct x, 0.001 z leakage, both. The vertical leakage is negligible in the measurement band except for spikes at the bounce and roll mode frequencies (17.5 and 25.0 Hz).

```
Show[xonly,zon1000only,bothtn]
```

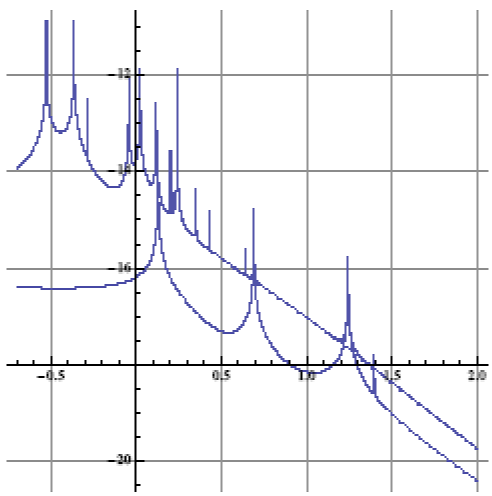

x thermal noise at the centre of the face for beamspitter with steel wires and 0.9° symmetric horizontal wedge rotated so that the front face is +x (20070718bswireHWsymrot), broken down by components: direct x, 0.01 z leakage, both. The vertical leakage dominates everywhere in the measurement band and is particularly bad at the bounce and roll mode frequencies (17.5 and 25.0 Hz).

```
Show[xonly,zon100only,bothtn100]
```

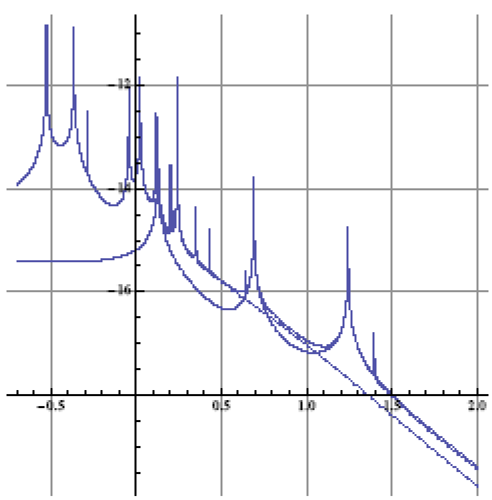

Figures 4 (upper) and 5 (lower). Thermal noise for BS on steel wires with a horizontal wedge and beam hitting centre of optic. Fig 4 assumes 0.001 z coupling and figure 5 assumes 0.01 z coupling.

x thermal noise at sweet spot in front of COM on front face (2.1 mm from centre) for beamspitter with steel wires and 0.9° symmetric horizontal wedge rotated so that the front face is +x (20070718bswireHWsymrot), broken down by components: direct x, 0.001 z leakage, both. The vertical leakage is negligible in the measurement band except for a large spike at the bounce mode frequency (17.5 Hz). The spike at the roll mode seen at the roll mode frequency (25.0 Hz) for a beam centred on the face is entirely suppressed.

`Show[xonlySS.zon1000onlySS.bothtnSS]`

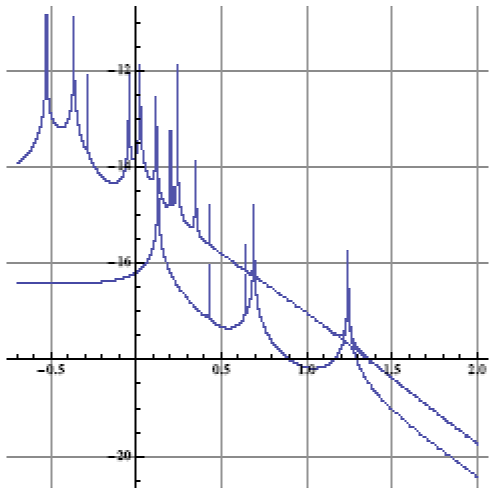

x thermal noise at sweet spot in front of COM on front face (2.1 mm from centre) for beamspitter with steel wires and 0.9° symmetric horizontal wedge rotated so that the front face is +x (20070718bswireHWsymrot), broken down by components: direct x, 0.01 z leakage, both. The vertical leakage dominates everywhere in the measurement band and is particularly bad at the bounce mode frequency (17.5 Hz). The spike at the roll mode seen at the roll mode frequency (25.0 Hz) for a beam centred on the face is entirely suppressed.

`Show[xonlySS.zon100onlySS.bothtn100SS]`

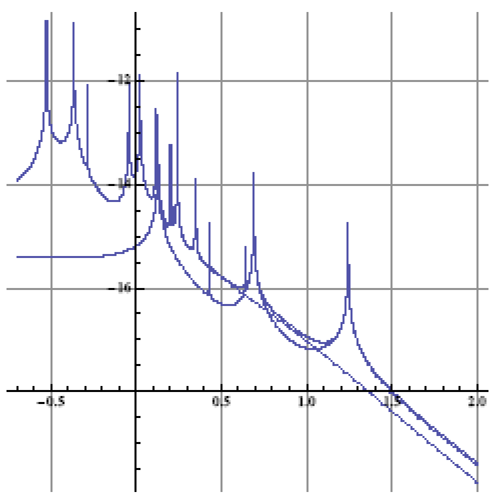

Figures 6 (upper) and 7 (lower). Thermal noise for BS on steel wires with a horizontal wedge and beam hitting sweet spot (see text).. Fig 6 assumes 0.001 z coupling and figure 7 assumes 0.01 z coupling.

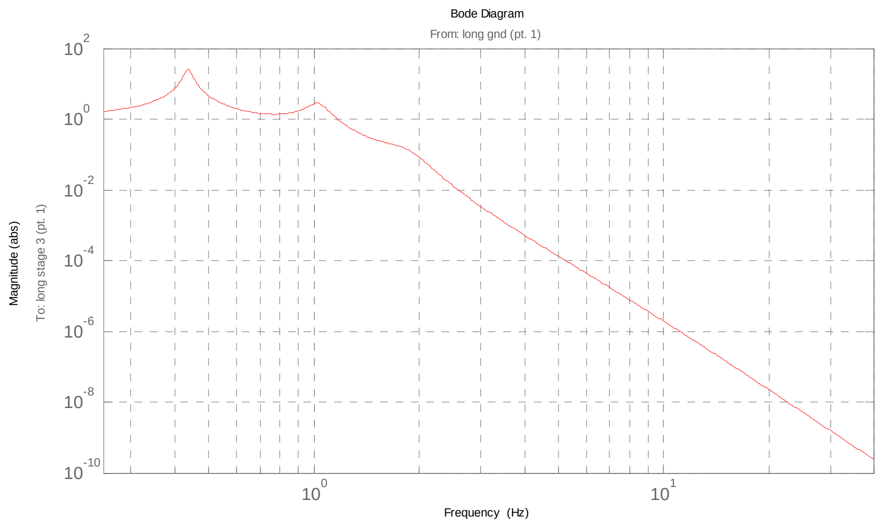

Figure 8. Horizontal (longitudinal) transfer function for beamsplitter triple suspension.

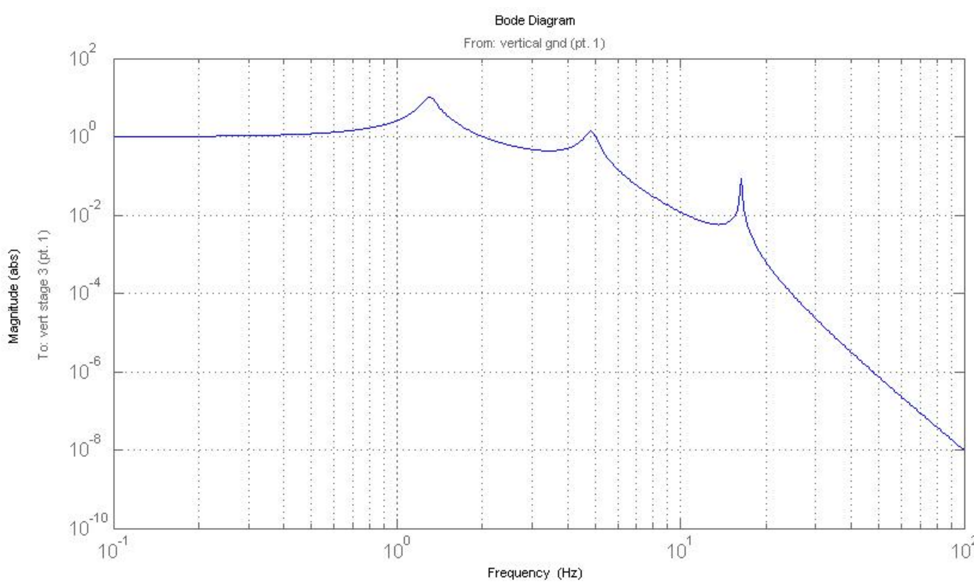

Figure 9. Vertical transfer function for beamsplitter triple suspension.

Appendix A

A.1 Summary of parameters used in the MATLAB code to generate figures 8 and 9.

```
        m1: 1.2627e+001
 material1: 'steel'
       I1x: 1.5472e-001
       I1y: 3.7733e-002
       I1z: 1.2456e-001
        m2: 1.4206e+001
 material2: 'silica'
        ix: 6.0000e-002
        ir: 1.8500e-001
       I2x: 2.4309e-001
       I2y: 1.2581e-001
       I2z: 1.2581e-001
        m3: 1.4206e+001
 material3: 'silica'
        tx: 6.0000e-002
        tr: 1.8500e-001
       I3x: 2.4309e-001
       I3y: 1.2581e-001
       I3z: 1.2581e-001
        l1: 5.2900e-001
        l2: 5.3000e-001
        l3: 6.0000e-001
       nw1: 2
       nw2: 4
       nw3: 4
        r1: 3.1100e-004
        r2: 1.8500e-004
        r3: 1.2900e-004
        Y1: 2.1190e+011
        Y2: 2.1190e+011
        Y3: 2.1190e+011
       l1b: 2.5000e-001
       a1b: 6.2500e-002
       h1b: 2.5000e-003
      ufc1: 2.7516e+000
       st1: 7.7297e+008
 intmode_1: 1.5059e+002
       l2b: 1.4000e-001
       a2b: 2.5333e-002
       h2b: 1.7000e-003
      ufc2: 3.1255e+000
```

```
                  st2: 7.9945e+008
            intmode_2: 3.2653e+002
                   su: 0
                   si: 1.5000e-002
                   sl: 5.0000e-003
                   n0: 7.7000e-002
                   n1: 1.3000e-001
                   n2: 6.0000e-002
                   n3: 1.9150e-001
                   n4: 1.8650e-001
                   n5: 1.8650e-001
               stage2: 1
                   d0: -1.7601e-003
                   d1: -5.9481e-004
                   d2: -5.9481e-004
                   d3: -1.5015e-004
                   d4: -1.5015e-004
                  tl1: 5.2458e-001
                  tl2: 5.1224e-001
                  tl3: 5.9970e-001
               l_cofm: 1.6365e+000
              l_total: 1.8215e+000
               ribbon: 0
                   db: 0
                    g: 9.8100e+000
                  kc1: 1.8872e+003
                  kc2: 2.7392e+003
l_suspoint_to_centreofoptic: 1.6365e+000
l_suspoint_to_bottomofoptic: 1.8215e+000
                flex1: 2.7601e-003
                flex2: 1.5948e-003
                flex3: 1.1501e-003
              flex3tr: 1.1501e-003
           longpitch1: [2.9665e-001 4.3614e-001 8.5846e-001]
           longpitch2: [1.0098e+000 1.2366e+000 1.8006e+000]
                  yaw: [5.3968e-001 1.5631e+000 2.1784e+000]
           transroll1: [4.3470e-001 1.0055e+000 1.6718e+000]
           transroll2: [2.5900e+000 4.0576e+000 2.3345e+001]
             vertical: [1.2872e+000 4.5671e+000 1.6383e+001]
```

These frequencies can be compared to those in the Mathematica model used for figures 1, 2, and 3 – see page 19. The differences (due to the shorter wire lengths used for the MATLAB model) are less than a few percent. The frequencies should also be compared with those given by the current (at time of writing) parameter set – see appendix C. The vertical and roll modes are slightly higher in Appendix C due to a shorter final stage in the suspension.

The top mass is represented above by a "T" shape with top plate (under which the 4 lower blades are attached as in the GEO and IMC designs) having dimensions in metres of ux = 0.06; uy= 0.44; uz= 0.0355, and the lower T section having dimensions vx= 0.06;vy = 0.08;vz = 0.142; all in steel, where x is longitudinal (perpendicular to face of optic) , y is transverse and z vertical.

The lower masses are at present represented by right circular cylinders of silica.

The blade design is outline only - needs to be refined using final size of mass (including wedge) and allowing for the correct "shape factor" for the size and shape of blades.

Appendix B

Parameters from Mark Barton's Mathematica code for steel wire case and 0.001 coupling (as used in figure 2) are shown below.

```
In[3]:= modelcase = "20070219bswire";

In[4]:= modelcasecomment = "The quad blade triple model xtra-lite beamsplitter. As for
        20060804bs but with improved Y1, Y2, r1, r2, wire damping, tmU, tmL, Csteel, Ysteel
        etc, plus steel wires in the final stage.";

In[5]:= Off[General::spell,General::spell1];
        overrides = {
            lockedblades->False, (* False for maximum realism. True for 100% Matlab
        compatibility *)
            kw1usual -> (Y1*A1)/l1,
            kw2usual -> (Y2*A2)/l2,
            kw3usual -> (Y3*A3)/l3,
            kbuzusual -> (m1/2)*(2*N[Pi]*ufc1)^2,
            kblzusual -> (m2/4)*(2*N[Pi]*ufc2)^2,
            kw1 -> If[lockedblades,recipadd[kw1usual, kbuzusual],kw1usual],
            kw2 -> If[lockedblades,recipadd[kw2usual, kblzusual],kw2usual],
            kw3 -> kw3usual,
            kbuz -> If[lockedblades,10^4*kbuzusual,kbuzusual],
            kblz -> If[lockedblades,10^4*kblzusual,kblzusual],
            kbuy -> If[lockedblades,10^4*kbuzusual,10^4*kbuzusual],
            kbly -> If[lockedblades,10^4*kblzusual,10^4*kblzusual],
            kbux -> If[lockedblades,10^4*kbuzusual,10^2*kbuzusual],
            kblx -> If[lockedblades,10^4*kblzusual,10^2*kblzusual],
            mbeu->0 (*If[lockedblades, 0.005/10^5, 0.005]*),
            mbel->0 (*If[lockedblades, 0.005/10^5, 0.005]*),

            den1->4000,
            ux->0.06,
            uy->0.44,
            uz->0.142,
            I1x ->1.5472 10^-001,
            I1y ->3.7733 10^-002,
            I1z ->1.2456 10^-001,
            m1 ->1.2627 10^+001,


            den2->2202,
            ix->0.06,
            ir->0.185,
            m2->den2*Pi* ir^2* ix,
            I2x->m2*(ir^2/2),
            I2y->m2*(ir^2/4+ix^2/12),
            I2z->m2*(ir^2/4+ix^2/12),


            tx->0.06,
            tr->0.185,
            den3->2202,
            m3->den3*Pi*tr^2*tx,
            I3x->m3*(tr^2/2),
            I3y->m3*(tr^2/4+tx^2/12),
            I3z->m3*(tr^2/4+tx^2/12),

            l1->0.55,
            l2->0.55,
            l3->0.60,

            r1->0.000311, (* copied from r1opt on preliminary run - Recurse[] hangs if
        substitution done directly *)
            r2->0.000185, (* copied from r2opt on preliminary run - Recurse[] hangs if
        substitution done directly *)
            r3->0.000129, (* copied from r3opt on preliminary run - Recurse[] hangs if
        substitution done directly *)

            bssteel -> 2*10^9, (* breaking stress of steel *)
            wssilica -> 7.7*10^8, (* working stress of silica *)
            r1opt->Sqrt[3*(m1+m2+m3)*g/nw1/c1/bssteel/N[Pi]],
            r2opt->Sqrt[3*(m2+m3)*g/nw2/c2/bssteel/N[Pi]],
            r3opt->Sqrt[3*(m3)*g/nw3/c3/bssteel/N[Pi]],
```

```
    Ysilica -> 7.0*10^10,

    Y1->Ysteel,
    Y2->Ysteel,
    Y3->Ysteel,

    ufc1->2.7516, (* copied from pend_ref.m output from triplep.m of 8/4/06 *)
    ufc2->3.1255, (* copied from pend_ref.m output from triplep.m of 8/4/06 *)

    d0->0.001-flex1,
    d1->0.001-flex2 (*+(g*m23)/(4*kblx)*),
    d2->0.001-flex2,
    d3->0.001-flex3,
    d4->0.001-flex3,
    su->0,
    si->0.015,
    sl->0.005,
    n0->0.077,
    n1->0.130,
    n2->0.060,
    n3->0.1915,
    n4->0.1865,
    n5->0.1865,

    flex1 -> Sqrt[nw1 M11 Y1/(m1+m2+m3)/g]*c1^(3/2),
    flex2 -> Sqrt[nw2 M21 Y2/(m2+m3)/g]*c2^(3/2),
    flex3 -> Sqrt[nw3 M31 Y3/m3/g]*c3^(3/2),

    rhosilica -> 2.2 10^3, (* IFOModel v4.1 *)
    Csilica -> 772., (* IFOModel v4.1 *)
    Ksilica -> 1.38,  (* IFOModel v4.1 *)
    alphasilica -> 5.1 10^-7, (* IFOModel v4.1 *)
    betasilica -> 1.52 10^-4, (* IFOModel v4.1 *)
    phisilica -> 4.1 10^-10, (* IFOModel v4.1 *)
    phissilica -> 3. 10^-11, (* surface *)
    dssilica -> 1.5 10^-2, (* IFOModel v4.1 *)

    rhosteel-> 7800., (* IFOModel v4.1 *)
    Csteel-> 486., (* IFOModel v4.? NAR 2/16/07 *)
    Ksteel-> 49., (* IFOModel v4.1 *)
    alphasteel-> 12. 10^-6, (* IFOModel v4.1 *)
    betasteel-> -2.5 10^-4, (* IFOModel v4.1 *)
    phisteel-> 2. 10^-4, (* Geppo's value  *)
    Ysteel -> 2.119 10^+11, (* measured, MB, 11/18/05, typo corrected *)

    rhomarag-> 7800., (* IFOModel v4.1 *)
    Cmarag-> 460., (* IFOModel v4.1 *)
    Kmarag-> 20., (* IFOModel v4.1 *)
    alphamarag-> 11. 10^-6, (* IFOModel v4.1 *)
    betamarag-> -2.5 10^-4, (* Geppo's value - Bench v4.1 is wrong *)
    phimarag-> 1. 10^-4, (* IFOModel v4.1 *)
    Ymarag-> 1.87 10^11, (* IFOModel v4.1 *)

    (* Zener, 1938, Phys. Rev. 53:90-99 *)
    magicnumber→1/4/FindRoot[0==D[BesselJ[1,x],x],{x,1.8}][[1,2]]^2,

    tmU-> 0.0025, (* upper blade thickness, NAR 8/4/06 *)
    tmL-> 0.0017, (* lower blade thickness, NAR 8/4/06 *)

    deltabladeU->Ymarag*alphamarag^2*temperature/(rhomarag*Cmarag), (* cf Bench
delta_v1 *)
    deltabladeL->Ymarag*alphamarag^2*temperature/(rhomarag*Cmarag), (* cf Bench
delta_v3 *)

deltawireU->Ysteel*temperature*(alphasteel-betasteel*g*(m1+m2+m3)/(nw1*N[Pi]*r1^2*Yste
el))^2/
           (rhosteel*Csteel), (* cf Bench delta_h1 *)

deltawireL->Ysteel*temperature*(alphasteel-betasteel*g*(m2+m3)/(nw2*N[Pi]*r2^2*Ysteel)
)^2
           /(rhosteel*Csteel), (* cf Bench delta_h3 *)
```

```
deltafibre->Ysteel*temperature*(alphasteel-betasteel*g*(m3)/(nw3*N[Pi]*r3^2*Ysteel))^2
           /(rhosteel*Csteel),

    taubladeU->rhomarag*Cmarag*tmU^2/(Kmarag*N[Pi]^2),
    taubladeL->rhomarag*Cmarag*tmL^2/(Kmarag*N[Pi]^2),
    tauwireU->magicnumber*rhosteel*Csteel*(2*r1)^2/Ksteel, (* cf Bench tau_steel1 *)
    tauwireL->magicnumber*rhosteel*Csteel*(2*r2)^2/Ksteel, (* cf Bench tau_steel3 *)
    taufibre->magicnumber*rhosteel*Csteel*4*(N[Pi]*r3^2)/N[Pi],

    damping[imag,bladeUtype] -> ((phimarag +
deltabladeU*(2*N[Pi]*#1*taubladeU)/(1+(2*N[Pi]*#1*taubladeU)^2))&),
    damping[imag,bladeLtype] -> ((phimarag +
deltabladeL*(2*N[Pi]*#1*taubladeL)/(1+(2*N[Pi]*#1*taubladeL)^2))&),
    damping[imag,wireUtype] -> (phisteel&),
    damping[imag,wireLtype] -> (phisteel&),
    damping[imag,wireUatype] -> ((phisteel +
deltawireU*(2*N[Pi]*#1*tauwireU)/(1+(2*N[Pi]*#1*tauwireU)^2))&),
    damping[imag,wireLatype] -> ((phisteel +
deltawireL*(2*N[Pi]*#1*tauwireL)/(1+(2*N[Pi]*#1*tauwireL)^2))&),
    damping[imag,fibretype] -> (phisteel&),
    damping[imag,fibreatype] -> ((phisteel +
deltafibre*(2*N[Pi]*#1*taufibre)/(1+(2*N[Pi]*#1*taufibre)^2))&)


};
On[General::spell,General::spell1]
```

```
g → 9.81
ux → 0.06
uy → 0.44
uz → 0.142
den1 → 4000
m1 → 12.627
I1x → 0.15472
I1y → 0.037733
I1z → 0.12456
ix → 0.06
ir → 0.185
den2 → 2202
m2 → 14.2057
I2x → 0.243095
I2y → 0.125809
I2z → 0.125809
tx → 0.06
tr → 0.185
den3 → 2202
m3 → 14.2057
I3x → 0.243095
I3y → 0.125809
I3z → 0.125809
l1 → 0.55
l2 → 0.55
l3 → 0.6
nw1 → 2
nw2 → 4
nw3 → 4
r1 → 0.000311
r2 → 0.000185
r3 → 0.000129
Y1 → 2.119×10^11
Y2 → 2.119×10^11
Y3 → 2.119×10^11
ufc1 → 2.7516
ufc2 → 3.1255
```

```
ufc3 → 0
d0 → -0.00176171
d1 → -0.000600407
d2 → -0.000600407
d3 → -0.00015015
d4 → -0.00015015
su → 0
si → 0.015
sl → 0.005
n0 → 0.077
n1 → 0.13
n2 → 0.06
n3 → 0.1915
n4 → 0.1865
n5 → 0.1865
tl1 → 0.545679
tl2 → 0.532848
tl3 → 0.5997
ltotal → 1.67823
leverarmrt → 0.03
leverarmrz → 0.08
leverarmrl → 0.08
gain → 0.4
gainrtzrtl → 0.4
gaint → 0.8
gainlrz → 0.4
b1 → 0.03
b2 → 0.03
b3 → 0.03
b4 → 0.03
b5 → 0.03
b6 → 0.03
unstretched → False
vertblades → True
ul1 → 0.548273
ul2 → 0.548268
ul3 → 0.598113
sl1 → 0.55
sl2 → 0.55
sl3 → 0.6
si1 → 0.0963636
si2 → 0.239091
si3 → 0.
c1 → 0.995346
c2 → 0.970997
c3 → 1.
pitchbul → 0
pitchbur → 0
pitchbll → 0
pitchblr → 0
pitchbllf → 0
pitchblrf → 0
pitchbllb → 0
pitchblrb → 0
rollbul → 0
rollbur → 0
rollbll → 0
rollblr → 0
rollbllf → 0
rollblrf → 0
```

---

rollbllb → 0
rollblrb → 0
A1 → 3.03858×10^{-7}
A2 → 1.07521×10^{-7}
A3 → 5.22792×10^{-8}
kw1 → 117068.
kw2 → 41424.9
kw3 → 18463.3
kbuz → 1887.12
kblz → 1369.62
bdu → 0.106667
bdl → 0.0508745
I1xy → 0
I1yz → 0
I1zx → 0
COM1x → 0
COM1y → 0
COM1z → 0
FRP1x → 0
FRP1y → 0
FRP1z → 0
Ibtxyl → 0
Ibtyzl → 0
Ibtzxl → 0
I2xy → 0
I2yz → 0
I2zx → 0
COM2x → 0
COM2y → 0
COM2z → 0
FRP2x → 0
FRP2y → 0
FRP2z → 0
I3xy → 0
I3yz → 0
I3zx → 0
COM3x → 0
COM3y → 0
COM3z → 0
FRP3x → 0
FRP3y → 0
FRP3z → 0
btx → 0.03
bty → 0.03
btz → 0.03
phib → 0.001
M11 → 7.34736×10^{-15}
M12 → 7.34736×10^{-15}
M21 → 9.19977×10^{-16}
M22 → 9.19977×10^{-16}
M31 → 2.17495×10^{-16}
M32 → 2.17495×10^{-16}
temperature → 290.
boltzmann → 1.38066×10^{-23}
alphasilica → 5.1×10^{-7}
betasilica → 0.000152
rhosilica → 2200.
Csilica → 772.

```
Ksilica → 1.38
Ysilica → 7. × 10^10
phisilica → 4.1 × 10^-10
phissilica → 3. × 10^-11
rhosteel → 7800.
Csteel → 486.
Ksteel → 49.
Ysteel → 2.119 × 10^11
alphasteel → 0.000012
betasteel → -0.00025
phisteel → 0.0002
rhomarag → 7800.
Cmarag → 460.
Kmarag → 20.
Ymarag → 1.87 × 10^11
alphamarag → 0.000011
betamarag → -0.00025
phimarag → 0.0001
tmU → 0.0025
tmL → 0.0017
magicnumber → 0.0737472
deltabladeU → 0.00182883
deltabladeL → 0.00182883
deltawireU → 0.0026483
deltawireL → 0.00264126
deltafibre → 0.00265023
taubladeU → 0.113606
taubladeL → 0.0525316
tauwireU → 0.0022073
tauwireL → 0.000781059
tausilica → 0.00833729
damping[imag, bladeUtype] → (0.0001 + (0.00130543 #1)/(1+0.509525 #1^2) &)
damping[imag, bladeLtype] → (0.0001 + (0.000603633 #1)/(1+0.108943 #1^2) &)
damping[imag, wireUtype] → (0.0002 &)
damping[imag, wireLtype] → (0.0002 &)
damping[imag, wireUatype] → (0.0002 + (0.0000367289 #1)/(1+0.000192346 #1^2) &)
damping[imag, wireLatype] → (0.0002 + (0.0000129621 #1)/(1+0.0000240839 #1^2) &)
damping[imag, fibretype] → (0.0002 &)
damping[imag, fibreatype] → (0.0002 + (0.00030987 #1)/(1+0.0136707 #1^2) &)
x00 → 0
y00 → 0
z00 → 0
yaw00 → 0
pitch00 → 0
roll00 → 0
kconx1 → 0
kcony1 → 0
kconz1 → 0
kconyaw1 → 0
kconpitch1 → 0
kconroll1 → 0
kconx2 → 0
kcony2 → 0
kconz2 → 0
kconyaw2 → 0
kconpitch2 → 0
kconroll2 → 0
```

```
kconx3 → 0
kcony3 → 0
kconz3 → 0
kconyaw3 → 0
kconpitch3 → 0
kconroll3 → 0
lockedblades → False
kw1usual → 117068.
kw2usual → 41424.9
kw3usual → 18463.3
kbuzusual → 1887.12
kblzusual → 1369.62
kbuy → 1.88712×10^7
kbly → 1.36962×10^7
kbux → 188712.
kblx → 136962.
mbeu → 0
mbel → 0
bssteel → 2000000000
wssilica → 7.7×10^8
r1opt → 0.000310741
r2opt → 0.000185102
r3opt → 0.000128975
flex1 → 0.00276171
flex2 → 0.00160041
flex3 → 0.00115015
dssilica → 0.015
taufibre → 0.0186087
```

N	f	type			
1	0.296631	pitch3	pitch2		
2	0.429032	y3	y2	roll3	
3	0.430418	x3	pitch3		
4	0.529992	yaw3	yaw2		
5	0.858447	pitch1	pitch3		
6	0.998615	y2	y3	roll3	roll2
7	1.00231	x2	x3	x1	
8	1.23617	pitch1			
9	1.28667	z3	z2		
10	1.54586	yaw1	yaw3		
11	1.651	roll3	roll2		
12	1.76682	x1			
13	2.15496	yaw2	yaw1		
14	2.57695	roll1	roll3		
15	4.05275	roll1			
16	4.56501	z1			
17	16.3825	z2	z3		
18	23.3453	roll2	roll3		

Thermal noise in x for beamspitter with steel wires (200701219bswire), broken down by components: direct x, 0.001 z leakage, both. The vertical leakage is negligible in the measurement band except for a spike at the bounce mode frequency (16.4 Hz).

Appendix C

Further update of parameter set and consideration of eddy current damping.

C.1 Modifications to parameter set.

i) Design of beamsplitter mass

There has been discussion on the actual thickness and wedge for the beamsplitter over the past few months, and several different parameter sets have been used while this conceptual design was being updated. At the time of finalising this revision (19th November 2007) RODA M070120-02 has been produced giving the design as follows: 370 mm diameter, horizontal symmetrical wedge with full wedge angle 0.9 degrees, thick end of wedge 60 mm thick, giving a mass of 13.5 kg. The mass is represented in the MATLAB model by assuming a thickness of the beamsplitter which is the average of the thin end and thick end of the wedge (Note that the MATLAB model assumes symmetry in the mass shapes). The penultimate mass has been modeled to be identical in mass and size, but will be made of metal with suitable holes to give the correct mass.

ii) Violin Mode Frequencies and Length of Wires

The SUS group has been asked by Peter F to consider shortening the length of the final stage of the suspension so that its violin mode frequency is higher than what would be obtained with the 600 mm length as given in Appendix A. By shortening to 500 mm and allowing a stress level of ~ 710 MPa (slightly more than the working value assumed for other Adv LIGO wire suspensions of 670 MPa) the frequency is raised from ~ 240 Hz to 300 Hz. Note that the use of steel rather than silica has reduced the expected violin mode frequency due to steel's higher density.

iii) Overall Length of Suspension

Ian W at RAL has indicated that a longer pendulum length could be incorporated within the same overall structure length by changing the way the top blade assembly is fixed within the structure compared to how this is done in the quad. The overall length of the pendulum could be increased by 66mm. Since this in principal gives a little more isolation, it has been used in the revised parameter set. The details on length are as follows

As per the following document, the optic table to optic CL (CL = centre line) for the ETM quad suspension is 1742 mm

http://www.eng-external.rl.ac.uk/advligo/Reviews/PDR3/documents/overview/t060142-00-k.pdf.

For the quad the length from tip of top blade to centre of optics is 1636 mm. Thus this allows 1742-1636 = 106 mm as space to fit in the blade supports and mount to the table in the quad. For the beamsplitter Ian is proposing that we can mount the blade tips closer to the table by 66 mm, so that they are now only 40 mm from the table. This means that we can make the overall length of the splitter from blade tip to centre of optic be 1636 + 66 = 1702 mm.

4) Top Mass

A detailed Solidworks design for the top mass has been put together by the RAL team. The conceptual T-shaped mass parameters have been replaced by the parameters from this detailed design.

With these changes the MATLAB parameter set and expected mode frequencies as of 19 Nov 2007 are as follows:

(taken from

C:\Documents and Settings\nroberts\My Documents\Caltech_work\MATLAB_at_Caltech\all triples\MB_BSmodel_Mar07_w_old_pendn\20070219BS)

Using Stage 2 fudges

Using matrix elements with no blade lateral compliance

Using matrix elements with quad blades at top mass

```
pend =

           m1: 1.2627e+001
    material1: 'steel'
          I1x: 1.6350e-001
          I1y: 2.4230e-002
          I1z: 1.6190e-001
           m2: 1.3517e+001
           ix: 5.7090e-002
           ir: 1.8500e-001
          I2x: 2.3130e-001
          I2y: 1.1932e-001
          I2z: 1.1932e-001
           m3: 1.3517e+001
    material3: 'silica'
```

tx: 5.7090e-002
tr: 1.8500e-001
I3x: 2.3130e-001
I3y: 1.1932e-001
I3z: 1.1932e-001
l1: 6.1200e-001
l2: 6.1000e-001
l3: 5.0000e-001
nw1: 2
nw2: 4
nw3: 4
r1: 3.1500e-004
r2: 1.8700e-004
r3: 1.2300e-004
Y1: 2.1190e+011
Y2: 2.1190e+011
Y3: 2.1190e+011
l1b: 2.5000e-001
a1b: 6.5000e-002
h1b: 2.4000e-003
ufc1: 2.8087e+000
st1: 7.7938e+008
intmode_1: 1.4457e+002
l2b: 1.4000e-001
a2b: 2.7556e-002
h2b: 1.6000e-003
ufc2: 3.2469e+000
st2: 7.8948e+008
intmode_2: 3.0733e+002
su: 0
si: 1.5000e-002
sl: 5.0000e-003
n0: 7.7000e-002

n1: 1.3000e-001
n2: 6.0000e-002
n3: 1.9150e-001
n4: 1.8650e-001
n5: 1.8650e-001
stage2: 1
d0: -1.8859e-003
d1: -6.9059e-004
d2: -6.9059e-004
d3: -7.1965e-005
d4: -7.1965e-005
tl1: 6.0781e-001
tl2: 5.9428e-001
tl3: 4.9986e-001
l_cofm: 1.7019e+000
l_total: 1.8869e+000
ribbon: 0
db: 0
g: 9.8100e+000
kc1: 1.9663e+003
kc2: 2.8127e+003
l_suspoint_to_centreofoptic: 1.7019e+000
l_suspoint_to_bottomofoptic: 1.8869e+000
flex1: 2.8859e-003
flex2: 1.6906e-003
flex3: 1.0720e-003
flex3tr: 1.0720e-003
longpitch1: [3.0258e-001 4.2554e-001 9.4183e-001]
longpitch2: [1.0410e+000 1.4855e+000 1.6624e+000]
yaw: [5.0122e-001 1.3672e+000 2.1890e+000]
transroll1: [4.2414e-001 1.0394e+000 1.5825e+000]
transroll2: [2.5848e+000 4.1031e+000 2.4986e+001]
vertical: [1.3368e+000 4.6494e+000 1.7531e+001]

Notes

1) The "d" values shown above are the actual positions of the break-off points to get an "effective" "d" value of 1 mm, taking into account the flexure lengths of the wires. The longitudinal compliance of the blades has not been included in this calculation. FEA models will be required to estimate the compliance and hence the revised positioning of the wire break-off points to compensate for that compliance.

2) There has been discussion of increasing the first pitch mode (currently 0.3 Hz) to decrease the overall rms motion of the optic. This can be done by increasing some of the "d" values and correspondingly decreasing wire lengths (to keep the overall height the same). This is ongoing work and is not reflected in the above parameter set.

3) The blade parameters and compliance are modeled using the opt.m routine. These should only be taken as representative and not the final design.

4) The penultimate mass and optic are represented in the MATLB model as being identical in mass size and moments of inertia. In addition they are represented as symmetric cylinders. In practice

i) the penultimate mass will be made of metal

ii) the optics will be horizontally wedged as described in C1 i) above. It is proposed that the penultimate mass is similarly wedged, and hung such that the wedged is oppositely oriented so that the overall loading on the blades above is symmetric.

Transfer functions using this parameter set, and assuming eddy current damping of the magnitude given in section C2 below, are shown in figures 10 and 11.

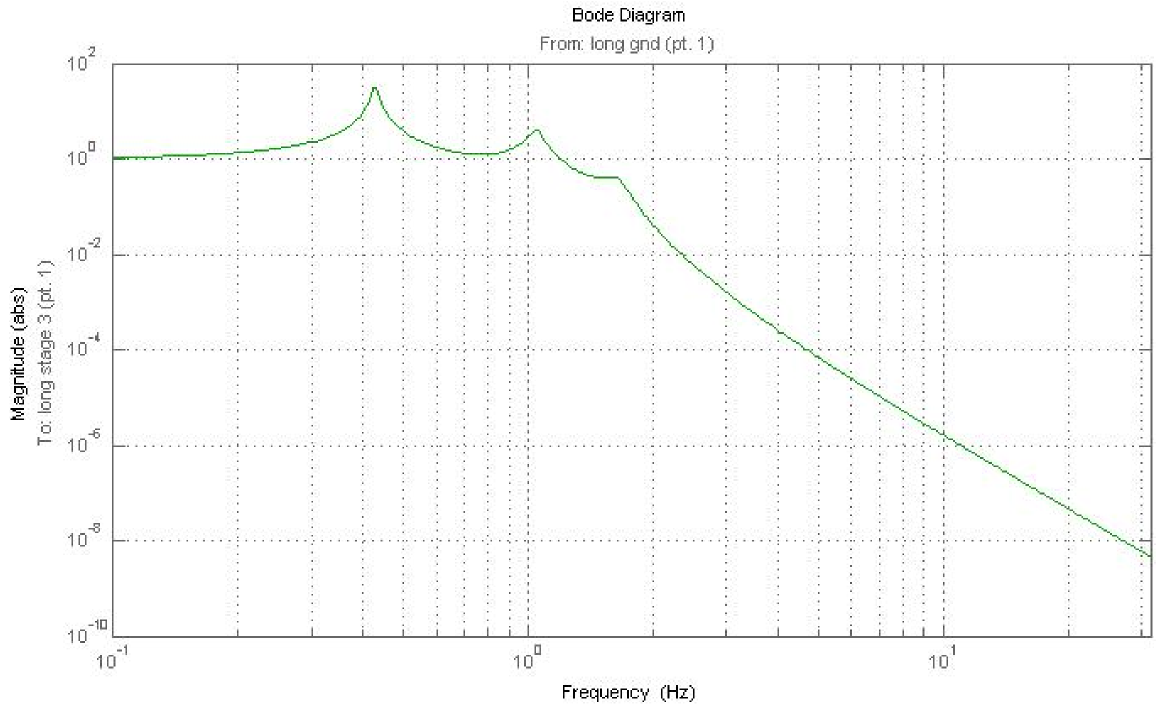

Figure 10 Longitudinal transfer function with parameter set given in appendix C, and using eddy current damping as in C2.

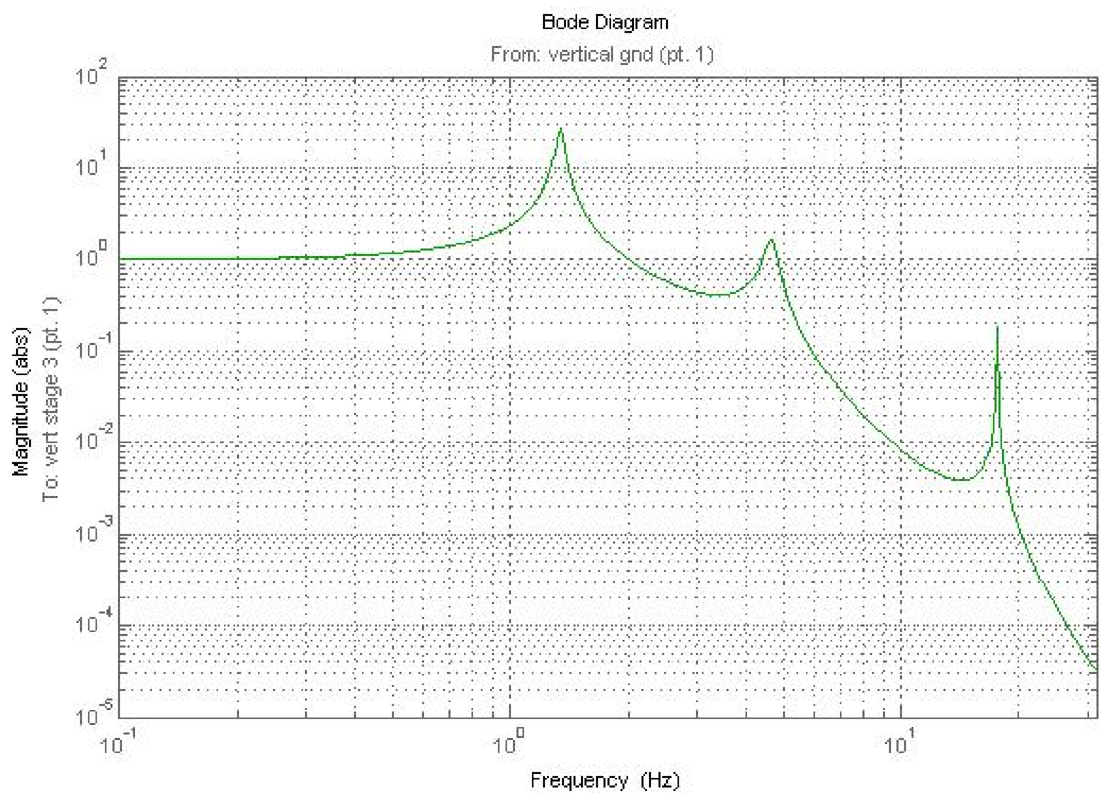

Figure 11 Vertical transfer function with parameter set given in appendix C, and using eddy current damping as in C2.

C2 Use of Eddy Current Damping.

In the current detailed design for the top mass ECD units similar to those being used in the ETM/ITM noise prototype are being incorporated. These units are arranged in clusters of 4 magnets (nominally 10 mm diam x 10 mm thick) with 4 such clusters acting in each of the longitudinal and vertical directions, arranged so that they also provide pitch, roll and yaw damping. Four clusters of four such magnets will give a damping constant of $b \sim 27$ kg/s (ref P060013-00-R). The transfer functions shown in figures 10 and 11 assume this value of b in longitudinal and vertical directions. The decay time to 1/e = 10.1 secs for longitudinal and 4.7 secs for vertical (we may choose to reduce magnet strength for this direction).

We can estimate the thermal noise due to this damping and show that it is acceptable. The noise force at the top mass where the damping is applied is given by F^2 = 4kTb, where k = Boltzmann's constant and T = temperature (K).

For b = 27 kg/s, F = 6.7 x 10^-10 N/rt Hz.

From the MATLAB model we find the following:

a) Longitudinal TF at 10 Hz for force at top mass to displacement of mirror, TF(long) =

8.7 x 10^-10 m/N.

Hence longitudinal motion due to thermal noise = F x TF(long) = 5.8 x 10^-19 m/rtHz.

b) Vertical TF at 10 Hz for force at top mass to displacement of mirror, TF(vert) =

1.9 x 10^-6 m/N.

Hence vertical motion due to thermal noise = F x TF(vert) = 1.3 x 10^-15 m/rtHz.

Assuming coupling of 0.1%, this gives longitudinal motion of

1.2 x 10^-18 m/rt Hz.

These values of longitudinal motion should be compared to the *technical* noise requirement for the beamsplitter of 2 x 10^-18 m/rtHz at 10 Hz. They are both below that value.